Maintenance of self-renewal ability of mouse embryonic stem cells in the absence of DNA methyltransferases Dnmt1, Dnmt3a and Dnmt3b

Akiko Tsumura[1,4], Tomohiro Hayakawa[2], Yuichi Kumaki[3,6], Shin-ichiro Takebayashi[1], Morito Sakaue[1], Chisa Matsuoka[1], Kunitada Shimotohno[4], Fuyuki Ishikawa[5], En Li[7], Hiroki R. Ueda[3], Jun-ichi Nakayama[2] and Masaki Okano[1,*]

[1]*Laboratory for Mammalian Epigenetic Studies,* [2]*Laboratory for Chromatin Dynamics, and* [3]*Laboratory for Systems Biology, Center for Developmental Biology, RIKEN, 2-2-3 Minatojima-Minamimachi, Chuo-ku, Kobe 650-0047, Japan*

[4]*Department of Viral Oncology, Institute for Virus Research, Kyoto University, 53 Kawaharacho, Shogoin, Sakyo-ku, Kyoto 606-8501, Japan*

[5]*Department of Gene Mechanisms, Graduate School of Biostudies, Kyoto University, Kitashirakawa-Oiwake-cho, Sakyo-ku, Kyoto 606-8502, Japan*

[6]*INTEC Web and Genome Informatics Corp., 1-3-3 Shinsuna, Koto-ku, Tokyo 136-8637, Japan*

[7]*Epigenetics Program, Novartis Institute for Biomedical Research, 250 Massachusetts Ave., Cambridge, MA 02139, USA*

DNA methyltransferases Dnmt1, Dnmt3a and Dnmt3b cooperatively regulate cytosine methylation in CpG dinucleotides in mammalian genomes, providing an epigenetic basis for gene silencing and maintenance of genome integrity. Proper CpG methylation is required for the normal growth of various somatic cell types, indicating its essential role in the basic cellular function of mammalian cells. Previous studies using *Dnmt1*$^{-/-}$ or *Dnmt3a*$^{-/-}$*Dnmt3b*$^{-/-}$ ES cells, however, have shown that undifferentiated embryonic stem (ES) cells can tolerate hypomethylation for their proliferation. In an attempt to investigate the effects of the complete loss of CpG DNA methyltransferase function, we established mouse ES cells lacking all three of these enzymes by gene targeting. Despite the absence of CpG methylation, as demonstrated by genome-wide methylation analysis, these triple knockout (TKO) ES cells grew robustly and maintained their undifferentiated characteristics. TKO ES cells retained pericentromeric heterochromatin domains marked with methylation at Lys9 of histone H3 and heterochromatin protein-1, and maintained their normal chromosome numbers. Our results indicate that ES cells can maintain stem cell properties and chromosomal stability in the absence of CpG methylation and CpG DNA methyltransferases.

Introduction

Vertebrate genomes are methylated on cytosines at levels much higher than those of other eukaryotic organisms, and are almost exclusively methylated at CpG dinucleotides (Bird 2002). CpG methylation plays an important role in epigenetic gene silencing and maintenance of genome stability, and is involved in a broad range of physiological and pathological processes in mammals, including embryogenesis, genome imprinting and tumorigenesis (Jones & Baylin 2002; Li 2002; Robertson 2005). In mice, three CpG DNA methyltransferases, Dnmt1, Dnmt3a and Dnmt3b, coordinately regulate CpG methylation in the genome (Li *et al.* 1992; Okano *et al.* 1999). Reduction of CpG methylation by inactivating these enzymes or related molecules in various mammalian cells results in growth defects, cell death, activation of retrotransposons and genome instability (Walsh *et al.* 1998; Xu *et al.* 1999; Jackson-Grusby *et al.* 2001; Rhee *et al.* 2002; Eden *et al.* 2003; Gaudet *et al.* 2003; Bourc'his & Bestor 2004; Dodge *et al.* 2005; Hata *et al.* 2006), indicating that CpG methylation plays a fundamental role in basic cellular functions of mammalian cells. Unlike differentiated somatic cells, undifferentiated ES cells can tolerate hypomethylation caused by inactivation of Dnmt1 or inactivation of both

Communicated by: Fumio Hanaoka
**Correspondence*: E-mail: okano@cdb.riken.jp

DOI: 10.1111/j.1365-2443.2006.00984.x

Dnmt3a and Dnmt3b for their proliferation (Lei *et al.* 1996; Chen *et al.* 2003; Jackson *et al.* 2004), indicating that gene silencing and chromatin structures are regulated differently in ES cells.

Post-translational modifications of specific amino acid residues of histones are also important for chromatin dynamics and epigenetic gene regulation (Jenuwein & Allis 2001). Functional relationships between CpG methylation and histone modification have been demonstrated in several species (Tamaru & Selker 2001; Jackson *et al.* 2002; Lehnertz *et al.* 2003; Tariq *et al.* 2003; Vire *et al.* 2006). Biochemical analyses have also shown that methyl-CpG-binding proteins interact with either histone deacetylases or histone methyltransferases (Jones *et al.* 1998; Nan *et al.* 1998; Ng *et al.* 1999; Wade *et al.* 1999; Zhang *et al.* 1999; Fujita *et al.* 2003; Sarraf & Stancheva 2004), further supporting the mechanistic links between these epigenetic mechanisms. Interestingly, a previous study using *Dnmt1*$^{-/-}$ and *Dnmt3a*$^{-/-}$*Dnmt3b*$^{-/-}$ ES cells showed that ES cells with a reduced level of CpG methylation maintain proper localization of the repressive chromatin markers histone H3 methylated at lysine 9 (H3K9) and heterochromatin protein-1 (HP1) at pericentromeric heterochromatin (Lehnertz *et al.* 2003), indicating that CpG methylation may contribute little to the regulation of higher-order chromatin structures in ES cells. That study, however, remains inconclusive because the mutant ES cells had residual CpG methylation and functional CpG methyltransferase activity.

In this study, we address whether mouse ES cells can survive in the absence of epigenetic regulation by CpG methylation, and if so, whether higher-order chromatin structures can be maintained in these cells. We established ES cells deficient for all three CpG methyltransferases, Dnmt1, Dnmt3a and Dnmt3b. We show that ES cells without CpG methylation maintain stem cell properties, proliferation ability, heterochromatic domains marked with H3K9 trimethylation, and euploidy.

Results

Establishment of Dnmt1/Dnmt3a/Dnmt3b triple knockout ES cells

We investigated the effects of the complete loss of CpG DNA methyltransferase function by inactivating *Dnmt1* via two rounds of gene targeting in *Dnmt3a*$^{-/-}$*Dnmt3b*$^{-/-}$ ES cells (Fig. 1A). This procedure yielded five independent clones of viable TKO *Dnmt1*$^{-/-}$*Dnmt3a*$^{-/-}$*Dnmt3b*$^{-/-}$ ES cells. We confirmed the accuracy of the gene targeting in these five cell lines by Southern blotting analysis (Fig. 1B and data not shown). Three of the five TKO cell lines were characterized in detail by Western blotting and RT-PCR analyses, showing the loss of gene products (Fig. 1B–D), and we used these for further studies.

Absence of CpG methylation in TKO ES cells

We evaluated the status of genome-wide CpG methylation in the TKO cells by several independent methods. We first examined CpG methylation of repetitive sequences by Southern hybridization using methylation-sensitive restriction enzymes. The methylation of two widely dispersed retroelement sequences, C-type endogenous retrovirus and intracisternal-A particles (IAP), was much lower in TKO cells as compared with *Dnmt1*$^{-/-}$ cells or *Dnmt1*$^{+/-}$*Dnmt3a*$^{-/-}$*Dnmt3b*$^{-/-}$ clones (Fig. 2A). In TKO cells, the digest patterns for CpG methylation-sensitive *Hpa*II and its CpG methylation-insensitive isoschizomer *Msp*I were indistinguishable, suggesting that CpG methylation in TKO cells was below the detection limit (Fig. 2A). Analysis of minor satellite repeats at centromeric regions and major satellite repeats at pericentromeric regions showed similarly reduced CpG methylation states in TKO cells (Fig. 2A).

We next examined the profiles and amounts of CpG methylation in TKO cells using bisulfite sequencing analysis, which can determine the exact sites of methylcytosine (Clark *et al.* 1994). Pericentromeric major satellite repeats, retroelement repeats, and the single-copy imprinted genes *Snrpn* and *Igf2r* all showed extensive loss of CpG methylation (Fig. 2B). We also sequenced random fragments of bisulfite-treated genomic DNA via shotgun sequencing and compared the sequences to the mouse genome (Table 1 and <http://www.dbsb.org/>). Two experiments using TKO cells showed that almost all methylcytosines were lost in 786 CpG sites over about 75 kb (Table 1). We detected a very small amount of methylcytosine-signals both at CpG sites (0.4%) and non-CpG sites (0.1–0.4%), possibly reflecting residual methylcytosines in the genome of TKO cells resulting from mechanisms other than methylation by Dnmt1/Dnmt3a/Dnmt3b. Such low levels, however, are nearly equivalent to the low frequency of experimental errors, including nucleotide misincorporation by Taq polymerase or incomplete bisulfite conversion. These data suggest that both CpG and non-CpG methylation in the TKO cells were below the limit of accuracy in our experimental procedures.

We then investigated the loss of CpG methylation at the cellular level by focusing on two cellular responses, localization of a methyl-CpG-binding protein and silencing of retroelements. To visualize the cytological distribution

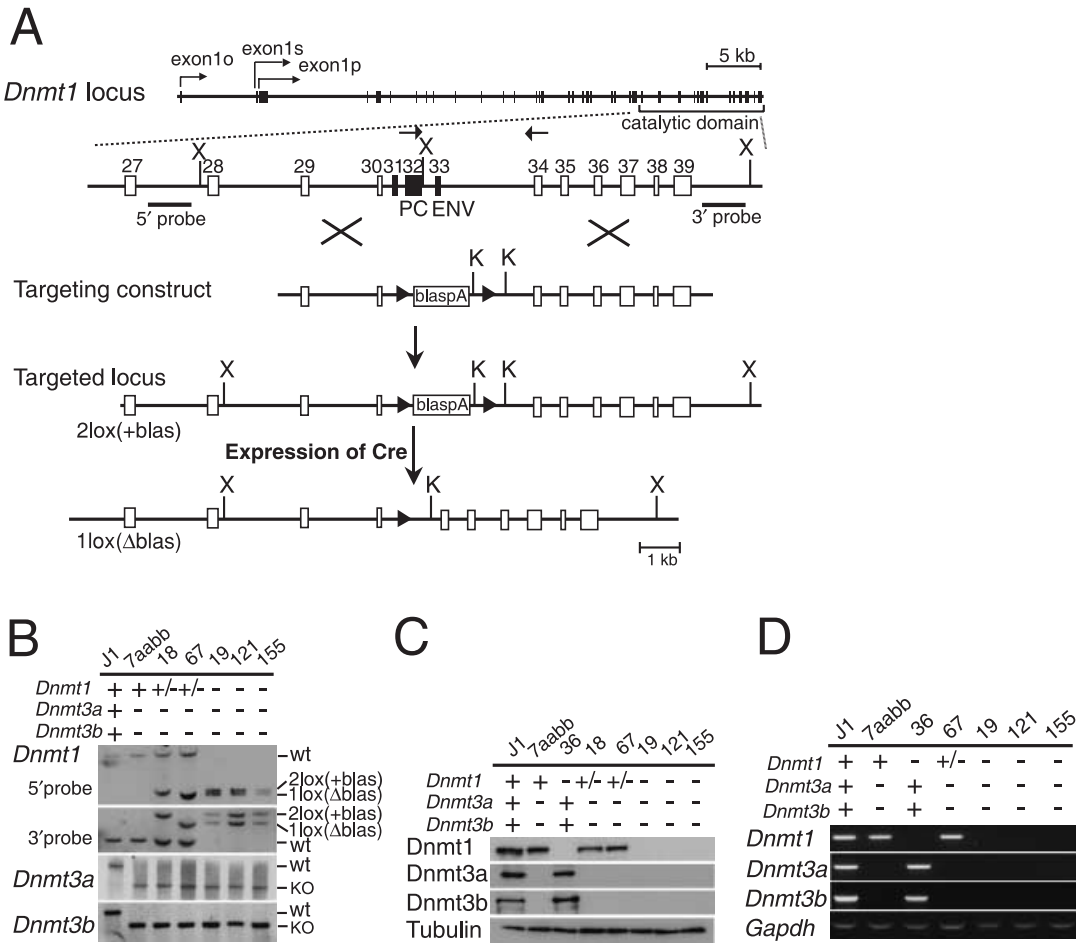

Figure 1 Generation of Dnmt1$^{-/-}$Dnmt3a$^{-/-}$Dnmt3b$^{-/-}$ ES cells. (A) Targeting of *Dnmt1* in *Dnmt3a*$^{-/-}$*Dnmt3b*$^{-/-}$ ES cells. To create a null allele, exons 31–33, encoding highly conserved Pro-Cys (PC) and Glu-Asn-Val (ENV) motifs, were replaced with the blasticidin resistance gene flanked with *loxP* sites (2lox(+blas)). Introduction of Cre excised the blasticidin resistance gene (1lox(Δblas)). The horizontal lines labeled "5′ probe" and "3′ probe" represent the two probes used for Southern blot analyses, and the arrows represent the primers used in the RT-PCR analysis. X, *Xba*I; K, *Kpn*I. (B–D) J1, wild-type line; 7aabb, *Dnmt3a*$^{-/-}$*Dnmt3b*$^{-/-}$ ES cell line; 36, a *Dnmt1*$^{-/-}$ ES cell line; 18 and 67, *Dnmt1*$^{+/-}$*Dnmt3a*$^{-/-}$*Dnmt3b*$^{-/-}$ parental lines of TKO ES cells with or without excision of the blasticidin gene by Cre (18, 2lox(+blas); 67, 1lox(Δblas)); 19, 121 and 155, independent *Dnmt1*$^{-/-}$*Dnmt3a*$^{-/-}$*Dnmt3b*$^{-/-}$ TKO lines. (B) Southern blot analysis of the mutant cell lines. Genomic DNA was digested with *Kpn*I (*Dnmt1*-5′probe), *Xba*I (*Dnmt1*-3′probe), *Hin*dIII (*Dnmt3a* probe) or *Bam*HI (*Dnmt3b* probe). wt, wild-type alleles; KO, mutant alleles; 2lox(+blas) and 1lox(Δblas), targeted *Dnmt1* alleles. (C) Western blot analysis of the mutant cell lines with anti-Dnmt1, anti-Dnmt3a or anti-Dnmt3b. Anti-tubulin was used as a control for equal protein loading. (D) RT-PCR analysis of the mutant cell lines with primers for *Dnmt1*, *Dnmt3a*, and *Dnmt3b*. Glyceraldehyde 3-phosphate dehydrogenase (*Gapdh*) was used as a control for equal RNA loading.

of CpG methylation in ES cells, we introduced and expressed green fluorescent protein fused to the methyl-CpG binding domain of MBD1 (GFP-MBD, Fujita *et al*. 1999). In interphase nuclei of wild-type and *Dnmt1*$^{-/-}$ ES cells, GFP-MBD mainly localized to pericentromeric heterochromatin regions that were densely stained by 4′,6′-diamino-2-phenylindole (DAPI). In contrast, GFP-MBD distribution was diffuse in TKO cell nuclei, and its localization was not restricted to pericentromeric heterochromatin (Fig. 2C), in agreement with our observation of extensive loss of CpG methylation at pericentromeric regions in these cells (Fig. 2A,B). We also examined the expression of two retroelements, IAP and LINE1, which are normally silenced and are de-repressed in severely hypomethylated embryos or germ cells (Walsh *et al*. 1998; Bourc'his & Bestor 2004; Hata *et al*. 2006). Consistent with the CpG methylation status of these retroelements (Fig. 2B), transcripts of

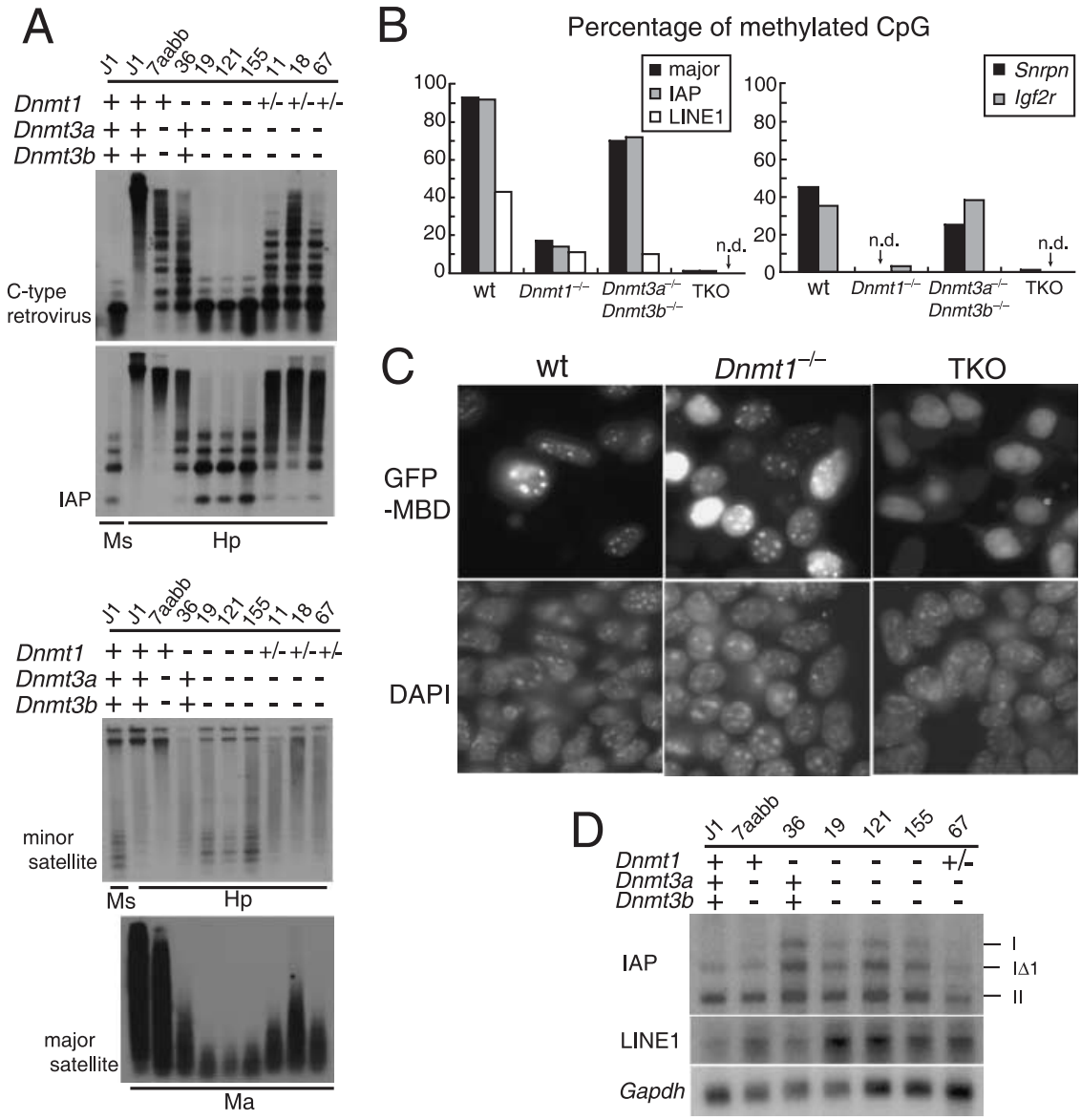

Figure 2 Extensive loss of CpG methylation in TKO cells. (A) DNA methylation of repetitive sequences as determined by Southern analysis of TKO cells. Genomic DNA was digested with CpG methylation–sensitive *Hpa*II (Hp) and *Mae*II (Ma) or CpG methylation–insensitive *Msp*I (Ms) and analyzed with probes against the following: C-type endogenous retrovirus, intracisternal-A particle retroelements (IAP), centromeric repeats (minor satellites), and pericentromeric repeats (major satellites). Clone 11 was a non-targeted clone during the second round of targeting of *Dnmt1*, which retained an intact *Dnmt1* allele and underwent the same number of passages as TKO cells. (B) DNA methylation analysis of repetitive sequences (pericentromeric major satellite repeats, IAP and LINE1; left) and imprinted genes (*Snrpn* and *Igf2r*; right) by bisulfite sequencing analysis. The percentages of methylcytosine signal out of total CpG sites analyzed in the sequenced clones are indicated. n.d., not detected. (C) Localization of GFP-MBD in interphase nuclei of ES cells. DNA was visualized by DAPI. (D) Northern blot analysis of poly(A)$^+$ RNA from the various ES cell lines using IAP and LINE1 probes. I and IΔ1, full-length transcripts and variant truncated transcripts of type I IAP; II, type II IAP.

IAP were elevated in both the TKO and the *Dnmt1*$^{-/-}$ ES cells, whereas transcripts of LINE1 were elevated mainly in TKO cells (Fig. 2D). These data are consistent with the absence of CpG methylation in the TKO cells.

Maintenance of stem cell properties in TKO ES cells

Despite the absence of CpG methylation, TKO cells retained the morphological features of undifferentiated

Table 1 Random bisulfite sequencing analysis. Random fragments of bisulfite-treated genomic DNA from the ES cell lines were sequenced, and the methylation status of each cytosine was determined by alignment with the mouse genome. Methylation status of clones that mapped to multiple loci in the mouse genome was based on the highest probability alignment with the genomic sequence.

	No. of clones	Total (bp)	No. of methylcytosines/total no. of sites			
			CpG	CpA	CpC	CpT
Wild-type	119	16327	112/136 (82%)	7/1117	3/779	6/1142
Dnmt3a$^{-/-}$*3b*$^{-/-}$	63	8541	11/72 (15%)	3/661	5/415	3/588
Dnmt1$^{-/-}$	112	15450	26/143 (18%)	8/1106	2/765	1/1057
TKO (#19)	383	57404	⋆2/559 (0.4%)	8/4125	11/2725	5/4011
TKO (#121)	127	17448	⋆1/227 (0.4%)	3/1296	4/1009	1/1201

⋆Three cytosines at CpG sites remained unconverted to uracil after the bisulfite reaction in the TKO cells, and two of the three cytosines were derived from clones that contained more than three unconverted cytosines at non-CpG sites. In these cases, all unconverted cytosines were clustered within a 20-bp palindromic sequence, indicating the possibility of incomplete conversion by the bisulfite reaction.

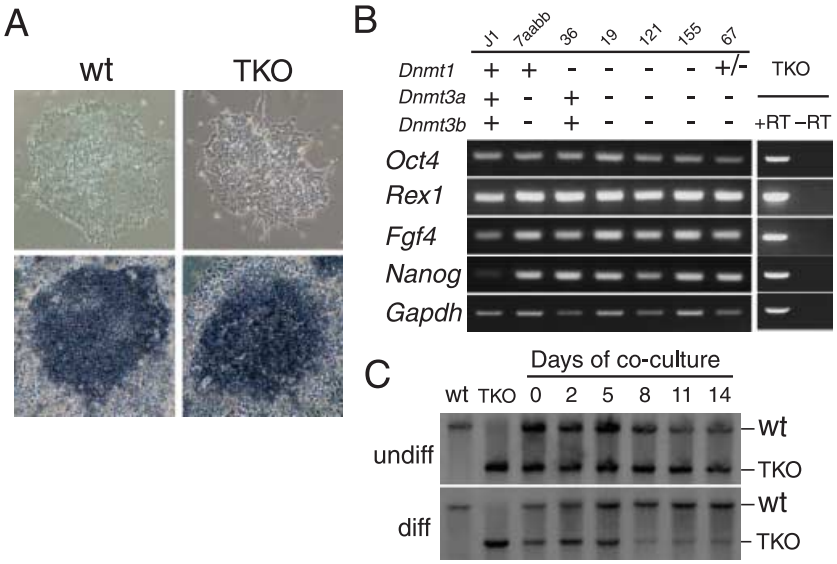

Figure 3 Maintenance of undifferentiated features in TKO cells. (A) Phase-contrast microscopic images (top) and alkaline phosphatase staining (bottom) of wild-type (wt) and TKO cells. (B) RT-PCR analysis of four representative undifferentiated ES cell markers, *Oct4*, *Rex1*, *Fgf4* and *Nanog*. No signal was observed in the negative control lacking reverse transcriptase (RT). (C) Growth competition in a mixture of wt and TKO cells under culture conditions that maintain the undifferentiated state (undiff, top) or promote differentiation (diff, bottom). Changes in the fraction of wild-type and TKO cells in the cell population at the indicated days were determined by Southern analysis using the *Dnmt3b* probe.

ES cells and stained positive for alkaline phosphatase activity, indicative of a pluripotent, undifferentiated state (Fig. 3A). TKO cells also expressed four other typical markers of undifferentiated cells (Oct4, Rex1, Fgf4 and Nanog) at the same or higher levels than wild-type ES cells (Fig. 3B). Growth curve experiments suggest that proliferation of undifferentiated TKO cells was comparable to, although slightly slower than, that of wild-type ES cells (Supplementary Fig. S1). We also estimated the growth rate of TKO cells by growth competition analysis, in which wild-type and TKO cells were cocultured, and the change in the fraction of wild-type and TKO cells in the cell population during the culture period was determined by Southern hybridization. The growth of undifferentiated TKO cells was comparable to that of wild-type cells, whereas their growth was delayed upon differentiation by formation of embryoid bodies (Fig. 3C), consistent with previous findings using *Dnmt1*$^{-/-}$ ES cells (Lei *et al*. 1996). These results suggest that CpG methylation is not essential for the self-renewal of ES cells in an undifferentiated state.

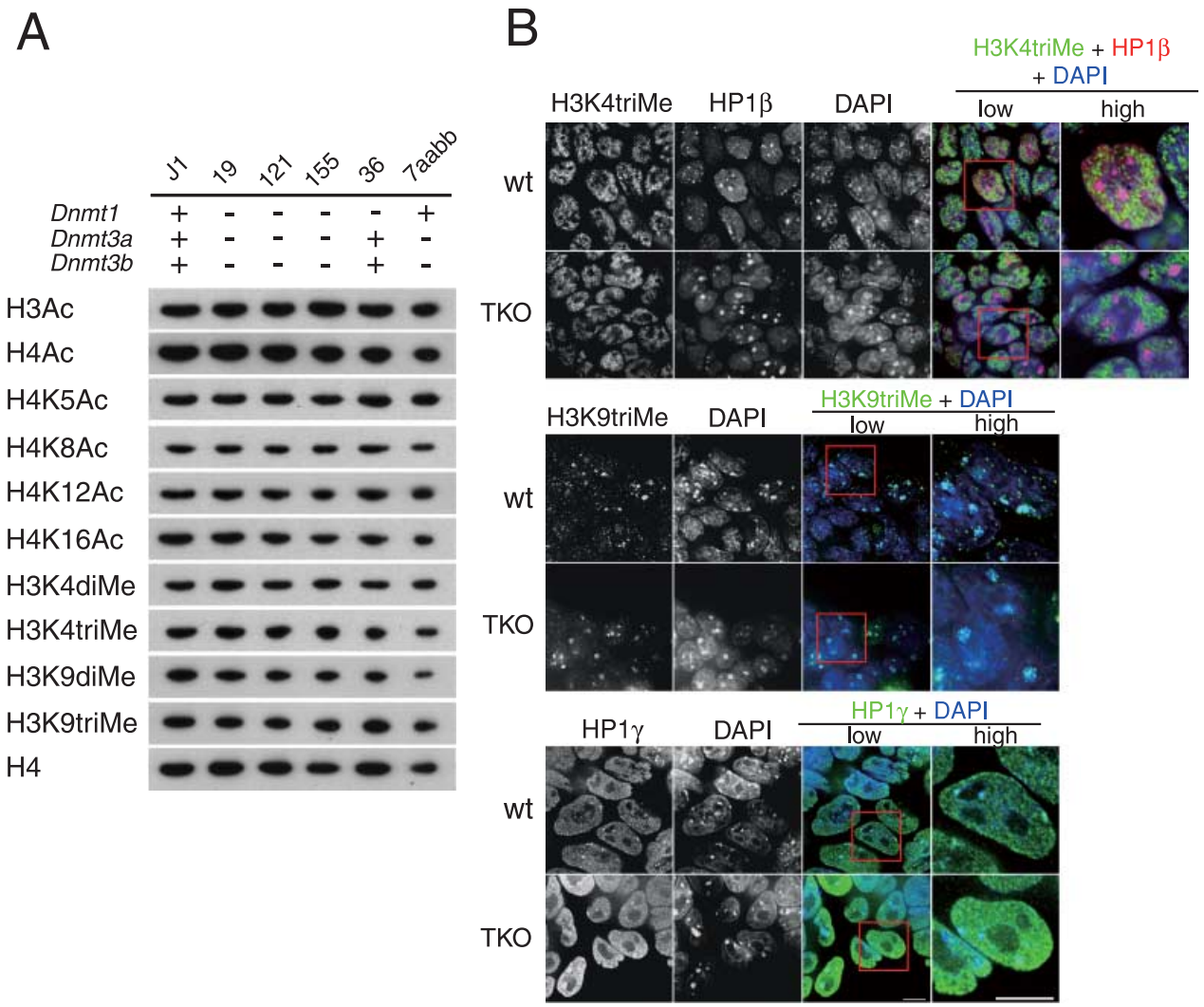

Figure 4 Maintenance of global chromatin structure in TKO cells. (A) Western blot analysis of global histone acetylation and methylation levels. H3Ac, acetylated histone H3; H4Ac, acetylated histone H4; H4K5Ac, H4K8Ac, H4K12Ac and H4K16Ac, acetylation at Lys5, Lys8, Lys12, or Lys16 of histone H4, respectively; H3K4diMe and H3K9diMe, dimethylation at Lys4 or Lys9 of histone H3, respectively; H3K4triMe and H3K9triMe, trimethylation at Lys4 or Lys9 of histone H3, respectively; H4, histone H4. Anti-histone H4 was used as a loading control. (B) Immunofluorescence analysis of interphase chromatin from wild-type (wt) and TKO cells using antibodies against trimethylated H3K9, trimethylated H3K4, HP1-β and HP1-γ. DNA was visualized with DAPI. Merged images represent overlays of immunofluorescence signal (green or red) and DAPI (blue) as indicated. "Low" and "high" indicate low and high magnification, respectively.

Maintenance of global chromatin structures in TKO ES cells

We next examined whether the absence of CpG methylation affects the post-translational modification of histone termini in ES cells. We assessed global histone acetylation and methylation by Western blotting using modification- and site-specific antibodies against histones H3 and H4. Acetylation at lysines of histones H3 and H4 and methylation at Lys4 of histone H3 (H3K4) are generally associated with transcriptionally active chromatin, whereas methylation at Lys9 of histone H3 (H3K9) is associated with transcriptionally repressed chromatin. Overall, the amounts of histone acetylation and methylation in TKO cells at most sites detected by the antibodies were similar to those in wild-type cells (Fig. 4A). We did not detect a significant increase in the acetylation of histone H4 at Lys5 in TKO cells, which was observed in *Dnmt3a*$^{-/-}$ *Dnmt3b*$^{-/-}$ ES cells of high passage numbers (Jackson *et al.* 2004).

We also investigated whether the absence of CpG methylation affects higher-order chromatin structure in ES cells. Trimethylation of H3K9 and co-localization of HP1 are characteristic features of pericentromeric heterochromatin, whereas methylation of H3K4 is normally absent in this region (Lehnertz *et al.* 2003; Maison & Almouzni 2004). Immunofluorescence analysis of TKO cells showed that the focal staining patterns of trimethylated H3K9 and HP1 overlapped with DAPI-dense heterochromatin regions, similar to the results for wild-type cells (Fig. 4B). The diffuse speckled patterns of trimethylated H3K4 found in TKO cell nuclei were also indistinguishable from those of wild-type cells (Fig. 4B). We did not observe a redistribution of H3K4 methylation to pericentromeric heterochromatin in TKO cells, as observed in hypomethylated mouse fibroblasts deficient for *Lsh* (Yan *et al.* 2003), a member of the SNF/helicase family involved in the control of global CpG methylation. Furthermore, analysis of metaphase chromosomes showed that TKO cells retained normal chromosomal number and banding patterns (Supplementary Fig. S2 and data not shown), indicating that condensation and segregation of chromosomes during mitosis occur properly in the absence of CpG methylation in ES cells.

Discussion

We have established the first mammalian cells deficient for the three known CpG DNA methyltransferases; CpG methylation is apparently absent in these cells. Our results provide direct genetic evidence that CpG methylation is dispensable for ES cell growth in an undifferentiated state, as suggested previously (Lei *et al.* 1996; Chen *et al.* 2003; Jackson *et al.* 2004). This stands in clear contrast to cases involving other cell types. Loss of *Dnmt1* in mouse embryonic fibroblasts leads to growth arrest associated with increased expression of *p21Waf1/Cip1* and *p57Kip2*, and *p53*-dependent cell death (Jackson-Grusby *et al.* 2001); moreover, the loss of both *DNMT1* and *DNMT3B* in human colon cancer cell lines causes growth impairment that is dependent on re-expression of *p16INK4A* (Rhee *et al.* 2002; Bachman *et al.* 2003). The unique cell cycle regulation of mouse ES cells (Hong & Stambrook 2004) may explain the robust growth and viability of our TKO cells.

Reduction of Dnmt1 activity in mice has been shown to induce tumors and chromosomal instability (Eden *et al.* 2003; Gaudet *et al.* 2003), and global hypomethylation in male germ cells results in meiotic abnormality (Bourc'his & Bestor 2004; Hata *et al.* 2006). Furthermore, inactivation of Dnmt3b in primary mouse embryonic fibroblast cells causes aneuploidy and chromosomal breaks and fusions (Dodge *et al.* 2005). These results suggest that proper CpG methylation level is important for chromosomal stability, at least in certain cell types. It remains unknown why undifferentiated ES cells retain chromosomal stability without CpG methylation and CpG DNA methyltransferases. One possibility is that ES cells maintain stable heterochromatin and chromosomes by an epigenetic mechanism that is independent of CpG methylation. Previous studies have shown that ES cells have both unique global chromatin modifications and heterochromatin arrangement, and that chromatin proteins bind more loosely to chromatin in ES cells than in differentiated cells, indicating the existence of specific epigenetic regulatory mechanisms in ES cells (Kimura *et al.* 2004; Meshorer *et al.* 2006). The absence or reduction of such mechanisms may be attributed to the chromosomal abnormality in differentiated cell types with decreased levels of CpG methylation. Taken together, these results suggest that the relative contribution of CpG methylation to both chromosomal stability and epigenetic gene silencing varies in a cell type-specific manner.

Our results suggest that at least some functional properties of heterochromatic domains are retained in the absence of CpG methylation in ES cells. However, it is possible that some unrecognized changes in heterochromatin occur in TKO cells. Indeed, the redistribution of the histone variant macroH2A into pericentromeric heterochromatin in hypomethylated *Dnmt1*$^{-/-}$ ES cells has recently been reported (Ma *et al.* 2005), indicating that CpG methylation modulates some properties of heterochromatic domains. Although the apparent contribution of CpG methylation to the steady-state heterochromatin structure in ES cells may be small, it is possible that CpG methylation might serve as a mark for anchoring heterochromatin during dynamic chromatin remodeling or during multiple replication processes. Further studies in this line are required for understanding the exact role of CpG methylation in higher-order chromatin structures.

The genomes of primordial germ cells and preimplantation embryos are extensively hypomethylated during normal embryogenesis (Hajkova *et al.* 2002; Li 2002), and global reduction of CpG methylation is a common feature of neoplasia (Feinberg *et al.* 2006). The generation of these triple methyltransferase-deficient ES cells will be useful in studying the role of CpG methylation in cell type-specific epigenetic regulation during normal and pathological processes. These cells will be also useful in investigating the function of chromatin modifications and remodeling in the absence of CpG methylation and endogenous CpG DNA methyltransferases in mammalian cellular conditions.

Experimental procedures

ES cell culture

ES cells were maintained in Glasgow modified Eagle medium (Sigma) supplemented with 15% foetal bovine serum, 0.1 mM nonessential amino acids (Invitrogen), 1 mM sodium pyruvate, 0.1 mM 2-mercaptoethanol and 2000 U/mL of leukemia inhibitory factor (LIF) and were grown on gelatinized culture dishes without feeder cells. For growth curve experiments, 0.9×10^5 ES cells were plated on gelatinized 10-cm culture dishes on the first day. Then, ES cells were passaged every 2 days with 6- to 12-fold dilution. For induction of differentiation by embryoid body formation, ES cells were seeded on low cell-binding dishes (Nunc) in medium without LIF. For growth competition analysis, wild-type and TKO cells were mixed at a 1 : 1 ratio and cultured either as undifferentiated ES cells or as embryoid bodies, as previously described (Lei *et al.* 1996). The change in cell population between wild-type and TKO cells was determined by Southern analysis using the *Dnmt3b* probe, which distinguishes between wild-type and TKO cells.

Generation of Dnmt1$^{-/-}$Dnmt3a$^{-/-}$Dnmt3b$^{-/-}$ ES cells

The following nucleotide positions of *Dnmt1* genomic DNA all refer to AC073775.2. The *Dnmt1* targeting vector, pTA009, was constructed by subcloning the 3-kb 5' arm (nt 66903–70025) and the 4-kb 3' arm (nt 71625–76570) of *Dnmt1* genomic DNA and a splicing acceptor–internal ribosomal entry site–blasticidin resistant gene cassette flanked by *loxP* sites (*loxP*-SAiresBlas-*loxP*) into pBluescript II SK. The *Dnmt1* genomic fragments were amplified by PCR from genomic DNA of ES cells (Supplementary Table S1). For targeting of the first *Dnmt1* allele, the *Dnmt1* targeting vector was transfected in *Dnmt3a*$^{-/-}$*Dnmt3b*$^{-/-}$ ES cells (Okano *et al.* 1999) via electroporation, and transfected cells were selected with 5 μg/mL blasticidin. Drug-resistant clones were screened by Southern hybridization using a 5′ probe (nt 65650–66729) and a 3′ probe (nt 76647–77192) external to the targeting construct (Fig. 1A). The targeting frequency was 14% (3/22). To generate blasticidin-sensitive ES cells, Cre recombinase was transiently expressed in blasticidin-resistant *Dnmt1*$^{+/-}$*Dnmt3a*$^{-/-}$*Dnmt3b*$^{-/-}$ ES cells (clone 18) by lipofection of a circular Cre expression plasmid. For targeting of the second wild-type Dnmt1 allele, the same targeting vector was transfected into blasticidin-sensitive *Dnmt1*$^{+/-}$*Dnmt3a*$^{-/-}$*Dnmt3b*$^{-/-}$ ES cells (clone 67), and the transfected cells were selected with 3.5 μg/mL blasticidin. Targeting frequency was 4% (5/113).

DNA methylation analysis

For Southern analysis, genomic DNA was digested with the CpG methylation-sensitive restriction enzymes *Hpa*II or *Mae*II (Roche), blotted and hybridized with probes specific for C-type endogenous retroviruses (pMO), IAP, minor satellite repeats, or major satellite repeats (Okano *et al.* 1999). For bisulfite sequencing analysis of specific sequences, 2 μg of genomic DNA digested with *Hin*dIII was treated with bisulfite followed by deamination (Clark *et al.* 1994). Deaminated fragments were amplified with primers for IAP, LINE1, major satellite repeats, *Igf2r* or *Snrpn* (Supplementary Table S1). We sequenced 15–30 clones for repetitive sequences and 9–15 clones for single-copy genes. Bisulfite sequencing of random genomic fragments was carried out as previously described (Ramsahoye *et al.* 2000). The sequences were aligned to the mouse genome sequence, NCBI Mouse Build 33 (Y.K. and H.R.U., unpublished data). Sequenced clones containing five non-CpG cytosines per sequenced clone that remained unconverted to uracil by the bisulfite reaction were excluded from the analysis. Overall, 80% of the sequenced clones longer than 51 bp could be mapped to the mouse genome. For localization of the methyl-CpG-binding protein, the GFP-MBD1(MBD+NLS) plasmid, which encodes an enhanced green fluorescent protein (EGFP) fused to the amino terminus of human MBD1 containing both a methyl-CpG-binding domain and a nuclear localization signal (Fujita *et al.* 1999; gift from M. Nakao), was transfected into the ES cells by Lipofectamine (Invitrogen). After 16 h of culture, the transfected cells were fixed with 4% paraformaldehyde and 0.5% [v/v] Triton X-100 in phosphate buffered saline (PBS) and were stained with DAPI.

RT-PCR and Northern blotting

RNA samples were isolated from subconfluent cells using the Trizol RNA extraction reagent (Invitrogen). Primer sets for *Dnmt1*, *Dnmt3a*, *Dnmt3b*, *Oct3/4*, *Rex1*, *Nanog*, *Fgf4* and *Gapdh* were used for RT-PCR (Supplementary Table S1). Poly(A)$^+$ RNA was prepared using the Poly(A) Tract purification system (Promega). Poly(A)$^+$ RNA (1 μg) was used for Northern analysis. The LINE1 probe was amplified by PCR (Supplementary Table S1).

Antibodies, Western blotting and immunofluorescence analysis

The following antibodies were used: anti-Dnmt1 (sc-20701) and anti-[acetyl-Lys5]H4 (sc8659-R) from Santa Cruz Biotechnology; anti-Dnmt3a (IMG-268) and anti-Dnmt3b (IMG-184) from IMGENEX; anti-α-tubulin (CP06) from Oncogene; anti-acetylated histone H3 (Lys9, Lys14; 06−599), anti-acetylated histone H4 (Lys5, Lys8, Lys12, Lys16; 06−866), anti-[acetyl-Lys8]H4 (17-211), anti-[acetyl-Lys12]H4 (17-211), anti-[acetyl-Lys16]H4 (06-762 and 07-329), anti-[dimethyl-Lys4]H3 (07−030), anti-[dimethyl-Lys9]H3 (07-212) and anti-histone H3 (06-755) from Upstate; anti-[acetyl-Lys16]H4 (ab1762), anti-[trimethyl-Lys4]H3 (ab8580) and anti-[trimethyl-Lys9]H3 (ab8898) from Abcam; and anti-HP1β (1MOD 1A9) and anti-HP1γ (2MOD 1G6) from EUROMEDEX. Alexa 488- and Alexa 546-conjugated secondary antibodies were purchased from Molecular Probes. A polyclonal antibody for Dnmt1 was raised against a modified linear peptide, CRESASAAVKAKEEAATKD, corresponding to the carboxy terminus of mouse Dnmt1. For Western blot analysis, whole-cell extracts were prepared by sonication in SDS-PAGE sample buffer, fractionated on an 8% SDS-PAGE gel and blotted using standard

procedures. Histones from ES cell nuclei were extracted with 0.2 mol/L H_2SO_4, precipitated with trichloroacetic acid (final concentration 25%), fractionated on an 18% SDS-PAGE gel and blotted in 10 mM CAPS (pH 11.0)/20% methanol. Indirect immunofluorescence staining was performed essentially as described (Lehnertz *et al.* 2003), with some modifications as follows. Wild-type and knockout ES cells were cultured in 35-mm glass-bottom dishes (MatTek) precoated with 0.2% gelatin in PBS. The cells were fixed with 2% formaldehyde in PBS, permeabilized with 0.1% sodium citrate containing 0.1% [v/v] Triton X-100 followed by incubation in blocking buffer (PBS, 2.5% BSA, 0.1% [v/v] Tween-20, 10% fetal bovine serum). Primary antibodies (diluted in blocking buffer) were added to fixed cells. After washing with PBS, 0.25% BSA, 0.1% [v/v] Tween-20, cells were re-fixed with 2% formaldehyde in PBS and then incubated with secondary antibody. After several washes with PBS, 0.1% [v/v] Tween-20, the stained cells were processed sequentially with 20%, 40%, 60% and 80% [v/v] glycerol in PBS containing 2.5% 1,4-diazobicyclo-(2,2,2)-octane (DABCO) for mounting. The 20% and 40% glycerol contained 0.5 μg/mL DAPI. Finally, cells were mounted in 90% glycerol in distilled water for microscopic observation. Fluorescence microscope images were acquired using a DeltaVision microscope system (Applied Precision). Three-dimensional optical section images were taken at 0.5-μm focus intervals and computationally processed using SoftWoRx software (Applied Precision).

Acknowledgements

We thank H. Niwa for the original SAiresBlas cassette, M. Nakao for the GFP-MBD plasmid, M. Oda for suggestions regarding ES cell characterization, and D. Sipp, M. Royle and S. Hayashi for critical reading. This work was supported in part by Grants-in-Aid from the Ministry of Education, Culture, Sports, Science, and Technology of Japan.

References

Bachman, K.E., Park, B.H., Rhee, I., *et al.* (2003) Histone modifications and silencing prior to DNA methylation of a tumor suppressor gene. *Cancer Cell* **3**, 89–95.

Bird, A. (2002) DNA methylation patterns and epigenetic memory. *Genes Dev.* **16**, 6–21.

Bourc'his, D. & Bestor, T.H. (2004) Meiotic catastrophe and retrotransposon reactivation in male germ cells lacking Dnmt3L. *Nature* **431**, 96–99.

Chen, T., Ueda, Y., Dodge, J.E., Wang, Z. & Li, E. (2003) Establishment and maintenance of genomic methylation patterns in mouse embryonic stem cells by Dnmt3a and Dnmt3b. *Mol. Cell. Biol.* **23**, 5594–5605.

Clark, S.J., Harrison, J., Paul, C.L. & Frommer, M. (1994) High sensitivity mapping of methylated cytosines. *Nucleic Acids Res.* **22**, 2990–2997.

Dodge, J.E., Okano, M., Dick, F., *et al.* (2005) Inactivation of *Dnmt3b* in mouse embryonic fibroblasts results in DNA hypomethylation, chromosomal instability, and spontaneous immortalization. *J. Biol. Chem.* **280**, 17986–17991.

Eden, A., Gaudet, F., Waghmare, A. & Jaenisch, R. (2003) Chromosomal instability and tumors promoted by DNA hypomethylation. *Science* **300**, 455.

Feinberg, A.P., Ohlsson, R. & Henikoff, S. (2006) The epigenetic progenitor origin of human cancer. *Nat. Rev. Genet.* **7**, 21–33.

Fujita, N., Takebayashi, S., Okumura, K., *et al.* (1999) Methylation-mediated transcriptional silencing in euchromatin by methyl-CpG binding protein MBD1 isoforms. *Mol. Cell. Biol.* **19**, 6415–6426.

Fujita, N., Watanabe, S., Ichimura, T., *et al.* (2003) Methyl-CpG binding domain 1 (MBD1) interacts with the Suv39h1-HP1 heterochromatic complex for DNA methylation-based transcriptional repression. *J. Biol. Chem.* **278**, 24132–24138.

Gaudet, F., Hodgson, J.G., Eden, A., *et al.* (2003) Induction of tumors in mice by genomic hypomethylation. *Science* **300**, 489–492.

Hajkova, P., Erhardt, S., Lane, N., *et al.* (2002) Epigenetic reprogramming in mouse primordial germ cells. *Mech. Dev.* **117**, 15–23.

Hata, K., Kusumi, M., Yokomine, T., Li, E. & Sasaki, H. (2006) Meiotic and epigenetic aberrations in *Dnmt3L*-deficient male germ cells. *Mol. Reprod. Dev.* **73**, 116–122.

Hong, Y. & Stambrook, P.J. (2004) Restoration of an absent G_1 arrest and protection from apoptosis in embryonic stem cells after ionizing radiation. *Proc. Natl. Acad. Sci. USA* **101**, 14443–14448.

Jackson, M., Krassowska, A., Gilbert, N., *et al.* (2004) Severe global DNA hypomethylation blocks differentiation and induces histone hyperacetylation in embryonic stem cells. *Mol. Cell. Biol.* **24**, 8862–8871.

Jackson, J.P., Lindroth, A.M., Cao, X. & Jacobsen, S.E. (2002) Control of CpNpG DNA methylation by the KRYPTONITE histone H3 methyltransferase. *Nature* **416**, 556–560.

Jackson-Grusby, L., Beard, C., Possemato, R., *et al.* (2001) Loss of genomic methylation causes p53-dependent apoptosis and epigenetic deregulation. *Nat. Genet.* **27**, 31–39.

Jenuwein, T. & Allis, C.D. (2001) Translating the histone code. *Science* **293**, 1074–1080.

Jones, P.A. & Baylin, S.B. (2002) The fundamental role of epigenetic events in cancer. *Nat. Rev. Genet.* **3**, 415–428.

Jones, P.L., Veenstra, G.C.J., Wade, P.A., *et al.* (1998) Methylated DNA and MeCP2 recruit histone deacetylase to repress transcription. *Nat. Genet.* **19**, 187–191.

Kimura, H., Tada, M., Nakatsuji, N. & Tada, T. (2004) Histone code modifications on pluripotential nuclei of reprogrammed somatic cells. *Mol. Cell. Biol.* **24**, 5710–5720.

Lehnertz, B., Ueda, Y., Derijck, A.A.H.A., *et al.* (2003) *Suv39h*-mediated histone H3 lysine 9 methylation directs DNA methylation to major satellite repeats at pericentric heterochromatin. *Curr. Biol.* **13**, 1192–1200.

Lei, H., Oh, S.P., Okano, M., *et al.* (1996) De novo DNA cytosine methyltransferase activities in mouse embryonic stem cells. *Development* **122**, 3195–3205.

Li, E. (2002) Chromatin modification and epigenetic reprogramming in mammalian development. *Nat. Rev. Genet.* **3**, 662–673.

Li, E., Bestor, T.H. & Jaenisch, R. (1992) Targeted mutation of the DNA methyltransferase gene results in embryonic lethality. *Cell* **69**, 915–926.

Ma, Y., Jacobs, S.B., Jackson-Grusby, L., *et al.* (2005) DNA CpG hypomethylation induces heterochromatin reorganization involving the histone variant macroH2A. *J. Cell Sci.* **118**, 1607–1616.

Maison, C. & Almouzni, G. (2004) HP1 and the dynamics of heterochromatin maintenance. *Nat. Rev. Mol. Cell Biol.* **5**, 296–304.

Meshorer, E., Yellajoshula, D., George, E., Scambler, P.J., Brown, D.T. & Misteli, T. (2006) Hyperdynamic plasticity of chromatin proteins in pluripotent embryonic stem cells. *Dev. Cell* **10**, 105–116.

Nan, X., Ng, H.H., Johnson, C.A., *et al.* (1998) Transcriptional repression by the methyl-CpG-binding protein MeCP2 involves a histone deacetylase complex. *Nature* **393**, 386–389.

Ng, H.H., Zhang, Y., Hendrich, B., *et al.* (1999) MBD2 is a transcriptional repressor belonging to the MeCP1 histone deacetylase complex. *Nat. Genet.* **23**, 58–61.

Okano, M., Bell, D.W., Haber, D.A. & Li, E. (1999) DNA methyltransferases Dnmt3a and Dnmt3b are essential for de novo methylation and mammalian development. *Cell* **99**, 247–257.

Ramsahoye, B.H., Biniszkiewicz, D., Lyko, F., Clark, V., Bird, A.P. & Jaenisch, R. (2000) Non-CpG methylation is prevalent in embryonic stem cells and may be mediated by DNA methyltransferase 3a. *Proc. Natl. Acad. Sci. USA* **97**, 5237–5242.

Rhee, I., Bachman, K.E., Park, B.H., *et al.* (2002) DNMT1 and DNMT3b cooperate to silence genes in human cancer cells. *Nature* **416**, 552–556.

Robertson, K.D. (2005) DNA methylation and human diseases. *Nat. Rev. Genet.* **6**, 597–610.

Sarraf, S.A. & Stancheva, I. (2004) Methyl-CpG binding protein MBD1 couples histone H3 methylation at lysine 9 by SETDB1 to DNA replication and chromatin assembly. *Mol. Cell* **15**, 595–605.

Tamaru, H. & Selker, E.U. (2001) A histone H3 methyltransferase controls DNA methylation in *Neurospora crassa*. *Nature* **414**, 277–283.

Tariq, M., Saze, H., Probst, A.V., Lichota, J., Habu, Y. & Paszkowski, J. (2003) Erasure of CpG methylation in *Arabidopsis* alters patterns of histone H3 methylation in heterochromatin. *Proc. Natl. Acad. Sci. USA* **100**, 8823–8827.

Vire, E., Brenner, C., Deplus, R., *et al.* (2006) The Polycomb group protein EZH2 directly controls DNA methylation. *Nature* **439**, 871–874.

Wade, P.A., Gegonne, A., Jones, P.L., Ballestar, E., Aubry, F. & Wolffe, A.P. (1999) Mi-2 complex couples DNA methylation to chromatin remodelling and histone deacetylation. *Nat. Genet.* **23**, 62–66.

Walsh, C.P., Chaillet, J.R. & Bestor, T.H. (1998) Transcription of IAP endogenous retroviruses is constrained by cytosine methylation. *Nat. Genet.* **20**, 116–117.

Xu, G.L., Bestor, T.H., Bourc'his, D., *et al.* (1999) Chromosome instability and immunodeficiency syndrome caused by mutations in a DNA methyltransferase gene. *Nature* **402**, 187–191.

Yan, Q., Huang, J., Fan, T., Zhu, H. & Muegge, K. (2003) Lsh, a modulator of CpG methylation, is crucial for normal histone methylation. *EMBO J.* **22**, 5154–5162.

Zhang, Y., Ng, H.H., Erdjument-Bromage, H., Tempst, P., Bird, A. & Reinberg, D. (1999) Analysis of the NuRD subunits reveals a histone deacetylase core complex and a connection with DNA methylation. *Genes Dev.* **13**, 1924–1935.

Received: 10 February 2006
Accepted: 12 April 2006

Supplementary material

The following supplementary material is available for this article online:

Figure S1 Growth curve analysis for TKO cells.

Figure S2 Chromosome analysis by Giemsa staining for TKO cells.

Table S1 Oligonucleotides used in this study.